J. Braz. Chem. Soc., Vol. 17, No. 8, 1634-1641, 2006.
Printed in Brazil - ©2006 Sociedade Brasileira de Química
0103 - 5053 $6.00+0.00

Article

A Novel Binuclear Ruthenium Complex: Spectroscopic and Electrochemical Characterization, and Formation of Langmuir and Langmuir-Blodgett Films

Karen Wohnrath,*[*,a] Poliana M. dos Santos,[a] B. Sandrino,[a] Jarem R. Garcia,[a] Alzir A. Batista[b] and Osvaldo N. Oliveira Jr.[c]

[a]*Departamento de Química, Universidade Estadual de Ponta Grossa, 84030-900 Ponta Grossa - PR, Brazil*

[b]*Departamento de Química, Universidade Federal de São Carlos, CP 676, 13565-905 São Carlos - SP, Brazil*

[c]*Instituto de Física de São Carlos, Universidade de São Paulo, CP 369, 13560-970 São Carlos - SP, Brazil*

O complexo [{$RuCl_3$(dppb)}$_2$(μ-4,4'-bipy)] (dppb = $PPh_2(CH_2)_4PPh_2$; 4,4'-bipy= 4,4'-bipiridil) foi obtido por meio da reação entre 4,4'-bipiridina e *mer*-[$RuCl_3$(dppb)]·H_2O, em bom rendimento. As características do complexo binuclear obtido, estudadas por medidas de FT-IR, UV-Vis, EPR e análise elementar foram similares às do complexo [$RuCl_3$(dppb)L] (L= N-heterociclo). [{$RuCl_3$(dppb)}$_2$(μ-4,4'-bipy)] é solúvel em solventes fracamente polares, facilitando a sua utilização para produzir filmes de Langmuir e Langmuir-Blodgett (LB). Enquanto que filmes *cast* e o complexo em solução são vermelhos, filmes LB são azul-esverdeados, provavelmente devido à oxidação da bisfosfina. A natureza nanoestruturada dos filmes LB, se manifestou nas medidas eletroquímicas, já que estes filmes exibem maior corrente de pico do que os filmes *cast* e *dip-coated*. As respostas eletroquímicas destes filmes são caracterizadas pelo processo $Ru^{III}Ru^{III}/Ru^{II}Ru^{II}$, o qual difere do complexo em solução. Neste último caso, um processo irreversível é observado devido à formação de novas espécies. A eletroatividade dos filmes LB/[{$RuCl_3$(dppb)}$_2$(μ-4,4'-bipy)] indica a possibilidade de utilização em dispositivos eletroquímicos.

[{$RuCl_3$(dppb)}$_2$(μ-4,4'-bipy)] was prepared from the reaction of the 4,4'-bipyridine and *mer*-[$RuCl_3$(dppb)]·H_2O, in good yield. The characteristics of the binuclear complex studied with FT-IR, UV-Vis, EPR and elemental analysis were similar to those of the [$RuCl_3$(dppb)L] (L= N-heterocycle). [{$RuCl_3$(dppb)}$_2$(μ-4,4'-bipy)] is soluble in weakly polar organic solvents, facilitating its use in the production of Langmuir and Langmuir-Blodgett (LB) films production. While the cast films and the complex in solution were red, the LB films were green-bluish, probably due to oxidation of the bisphosphine. The nanostructured nature of the LB films was manifested in electrochemical measurements, as these films exhibited higher peak currents than cast or dip-coated films. For all films, the electrochemical response was dominated by the $Ru^{III}Ru^{III}/Ru^{II}Ru^{II}$ process, which differed from that of the binuclear compound. For the latter, an irreversible process appeared due to formation of new species. The electroactivity of LB films from [{$RuCl_3$(dppb)}$_2$(μ-4,4'-bipy)] also pointed to their possible use in electrochemical devices.

Keywords: binuclear ruthenium complexes, bipyridine, Langmuir-Blodgett films, thin films

Introduction

Ordered films of transition-metal complexes have large potential for various applications, including electrochemical devices, which requires the understanding of their electrical and structural properties.[1,2] For ruthenium complexes, in particular, Langmuir-Blodgett films (LB films) may be used in electrochemical sensors,[3-5] molecular devices,[6] electronic tongues,[7-9] electroluminescence devices[10,11] and as redox-active and photo-induced sensitizers.[12,13] This variety of properties arises from the possibility of tuning the electronic and electrochemical characteristics of the ruthenium complex, mostly through changes in the ligand linked to the central metal. Ligands with low-energy π electrons may be coupled to metal ions with various redox states.[14] Phosphine ligands may exhibit varied steric and electronic properties that can be used to modify the oxidation chemistry of ruthenium complexes.[15] In addition phosphines may stabilize isolated compounds or intermediates in homogeneous catalysis[16,17] and in chemotherapy agents.[18]

The final properties of LB films depend on the molecular architecture, in addition to the complex

*e-mail: kawoh@uepg.br

characteristics determined by the choice of the ligand. This has motivated several works on organized structures containing metal complexes, in monolayers,[19-22] one-dimensional rods and tubules.[23] Ruthenium complexes with the Ru-PP core, where PP is a biphosphine, could form stable monolayers in water, as was the case of *mer*-[$RuCl_3$(dppb)L] (dppb= $PPh_2(CH_2)_4PPh_2$; L= pyridine and 4-methylpyridine), named as Rupy and Rupic, respectively.[24-27] The molecular organization was extracted from the information provided by surface pressure-molecular area (π-*A*) isotherms, atomic force microscopy (AFM), UV-vis absorption, FT-IR, reflection-absorption infrared spectroscopy (RAIRS), Raman scattering, and fluorescence.[4,27,28] Rupic immobilized in LB film is useful for the selective oxidation of dopamine and ascorbic acid, and yielded more reproducible surfaces in comparison with carbon paste.[4]

The possible applications for Rupic and Rupy LB films just described motivated us to seek other synthetic routes that could lead to novel functional materials. We selected the mixed-valence chemistry[29-31] of polynuclear transition metals, which has been widely used by inorganic chemists[32] to obtain properties that may be tuned *via* specific interactions at the molecular level and/or quantum confinement. In this paper, we present a detailed study of the binuclear complex, [{$RuCl_3$(dppb)}$_2$(μ-4,4'-bipy)] (4,4'-bipy= 4,4'-bipyridine), used in the fabrication of Langmuir and LB films whose properties will be compared to those of a mononuclear derivative.

Experimental

Chemicals and solvents

Reagent-grade chemicals were used without further purification while the reagent-grade solvents were distilled and dried before use. Purified argon was used for the elimination of dissolved oxygen in the solvents.

Preparation of [{$RuCl_3$(dppb)}$_2$(μ-4,4'-bipy)]

The complex [{$RuCl_3$(dppb)}$_2$(μ-4,4'-bipy)] was prepared from *mer*-[$RuCl_3$(dppb)]·H_2O[33] (100 mg, 1.53 mmol), and 4,4'-bipyridine (Aldrich) (11.9 mg, 0.076 mmol) in degassed dichloromethane (Merck) (10 mL) The reaction mixture was stirred for 12 h at room temperature. The volume of the resulting red solution was reduced *in vacuo* to *ca.* 2 mL and diethyl ether (Merck) was then added to precipitate a red solid which was filtered off, washed several times with diethyl ether and dried under vacuum. Yield: 81 mg (75%). Anal. Calc. for $C_{66}H_{64}N_2Cl_6P_{42}Ru_2$: C, 55.67; H, 4.53; N, 1.97%. Found: C, 56.27; H, 4.37; N, 1.56%. IR ν_{max}/cm^{-1}: $\nu_{(P-C)}$= 513, 999, 1095, 1485; $\gamma_{(C-H)}$= 696; $\nu_{(Ru-Cl)}$= 241 and 335. UV-vis: λ_{max}/nm (ε = mol^{-1} L cm^{-1}): 236 (4.55×10^4), 256 (4.90×10^4), 328 (5.25×10^3), 444 (1.12×10^3), 532 (1.76×10^3). EPR: g_1= 2.893, g_2= 2.124, g_3= 1.685.

Langmuir monolayers

Langmuir monolayers of [{$RuCl_3$(dppb)}$_2$(μ-4,4'-bipy)] were spread from chloroform (Merck) solutions on aqueous subphases, with ultra pure water supplied by a Millipore system with resistivity of 18.2 MΩ cm, in a KSV5000 Langmuir trough in a class 10,000 clean room. Surface pressure and surface potential of the monolayer were measured using a Wilhelmy plate connected to an electrobalance and a Kelvin probe, respectively, both provided by KSV. In all experiments, carried out at room temperature of 22 °C, 15 min elapsed before compression for solvent evaporation. The speed of barrier compression was 10 mm min^{-1}, and monolayer stability was investigated by monitoring the area change at a fixed pressure (25 mN m^{-1}) for *ca.* 10 min until the monolayer was stable, which was denoted by no change in area per molecule. The monolayers were transferred as Y-type LB films at 25 mN m^{-1} onto glass, ITO (tin oxide doped with indium, Asahi Glass Co.) and Si substrates (2 mm thick, diameter 13 mm, from Aldrich), depending on the characterization technique to be applied to the sample, as specified below. The dipping speed was 3 mm min^{-1} for the withdrawal and immersion of the substrate, with a waiting time of 5 min, when the substrate was out of the water, before the next layer was transferred. Transfer ratios were TR = 0.9 for downstrokes and 0.8 for upstrokes.

Physical measurements

The IR spectra of the powdered complex were recorded from CsI pellets in the 4000-200 cm^{-1} region and the IR spectra of the LB films were recorded from films with 61 monolayers deposited onto Si wafers. These measurements were performed with a Bomen Michelson FT spectrometer, model MB 102. The UV-Vis spectra of the complex in dichloromethane solution and the LB films, deposited with 31monolayers onto quartz substrate, were recorded with a HP 8452A and Shimadzu MultiSpec 1501 spectrophotometer, respectively. Elemental analyses were performed in a Fison EA 1108 model. The electron paramagnetic resonance spectrum in the solid state was measured at 160 °C using a Varian E-109 instrument operating at the X band frequency, within a rectangular cavity (E-248) fitted with a temperature controller.

Cyclic voltammetry (CV) experiments of the complex in solution were obtained in a BAS-100B/W Bioanalytical Systems Instrument. These experiments were carried out at room temperature in CH_2Cl_2 containing 0.10 mol L^{-1} $Bu_4N^+ClO_4^-$ (TBAP) (Fluka Purum) as support electrolyte using a one-compartment cell where the working and auxiliary electrodes were stationary Pt foils, and the reference electrode was Ag/AgCl, 0.10 mol L^{-1} TBAP in CH_2Cl_2, a medium in which ferrocene is oxidized at 0.43 V (Fc^+/Fc). The electrochemical measurements of LB films were carried out in a Microquimica MQPG-01 potentiostat, using a 10 mL electrochemical cell with the conventional three-electrode system: a Pt wire as a counter electrode, an Ag/AgCl in $KCl_{(sat.)}$ electrode as the reference and the LB film onto ITO as working electrodes. The measurements were made in the potential range between -0.1 V and 0.7 V, with scan rates of 30 mV s^{-1} and 50 mV s^{-1}. The electrochemical properties of the modified electrodes were studied with cyclic voltammetry in 0.5 mol L^{-1} KCl solutions at different pHs, adjusted with HCl or KOH. Redox potentials (E½) were determined from the average of the anodic and cathodic peak potentials (Epa and Epc).

Results and Discussion

Synthesis of the binuclear Ru complex

The reaction of the *mer*-$[RuCl_3(dppb)].H_2O$[33] complex with the free ligand, 4,4'-bipyridine in methylene chloride was used to prepare the binuclear complex of general formula $[\{RuCl_3(dppb)\}_2(\mu\text{-}4,4'\text{-bipy})]$, as a dark red powder, and with good yield. The *mer*-$[RuCl_3(dppb)].H_2O$ complex has been used as aprecursor to prepare compounds containing Ru^{III}P-P and Ru^{II}P-P cores,[34-37] in which the P-P ligand replaced chloride ligands. The elemental analysis of the red powder obtained after filtration demonstrated that no further purification was necessary. For the synthetic method described herein, only a slight excess of ligand (0.5 equiv.) was needed to prepare $[\{RuCl_3(dppb)\}_2(\mu\text{-}4,4'\text{-bipy})]$, owing to the strong chelate effect of the 4,4'-bipy ligand. Displacement of one chloride ligand was also observed by refluxing *mer*-$[RuCl_3(dppb)]\cdot H_2O$ in methylene chloride solution, for the formation of the same product. Other complexes can be formed using different stoichiometric quantities of the 4,4'-bipy ligand, as shown in Scheme 1. The nature of the products formed from the reaction of *mer*-$[RuCl_3(dppb)].H_2O$ with 4,4'-bipy depended on the complex to ligand ratio. For example, when a slight excess of ligand (1.1 equiv.) or an excess of ligand (2 equiv.) was added to the starting complex, the mononuclear, $[RuCl_3(dppb)(4,4'\text{-bipy})]$, or the tetramer complex $\{[Ru^{II}Cl_2(dppb)](\mu\text{-}4,4'\text{-bipy})\}_4$[38] were formed, respectively.

Spectroscopic characterization

The IR spectrum of the $[\{RuCl_3(dppb)\}_2(\mu\text{-}4,4'\text{-bipy})]$ complex obtained in CsI pellet (see Figure 1) displays the typical bands of the coordinated ligand at 1485, 1095, 999, and 513 ($\nu_{(P\text{-}C)}$), 696 ($\gamma_{(C\text{-}H)}$), 335 and 241 cm^{-1} ($\nu_{(Ru\text{-}Cl)}$).[39] The presence of a Ru^{III} species was confirmed by EPR measurements, with the spectrum in Figure 2 showing g values (g_1= 2.893, g_2= 2.124, g_3= 1.685) typical of Ru^{III} complexes with strong rhombic distortions.[34, 39,40] The spectrum is similar to that of the mononuclear pyridine species with general formula $[RuCl_3(dppb)L]$ (L= pyridine) (g_1= 2.928, g_2= 2.037, g_3= 1.607).[34] This is a strong indication that the additional "$RuCl_3$(P-P)" core, in the binuclear complex, has no effect in the rhombic distortions of the Ru^{III}-N-N-Ru^{III} core.

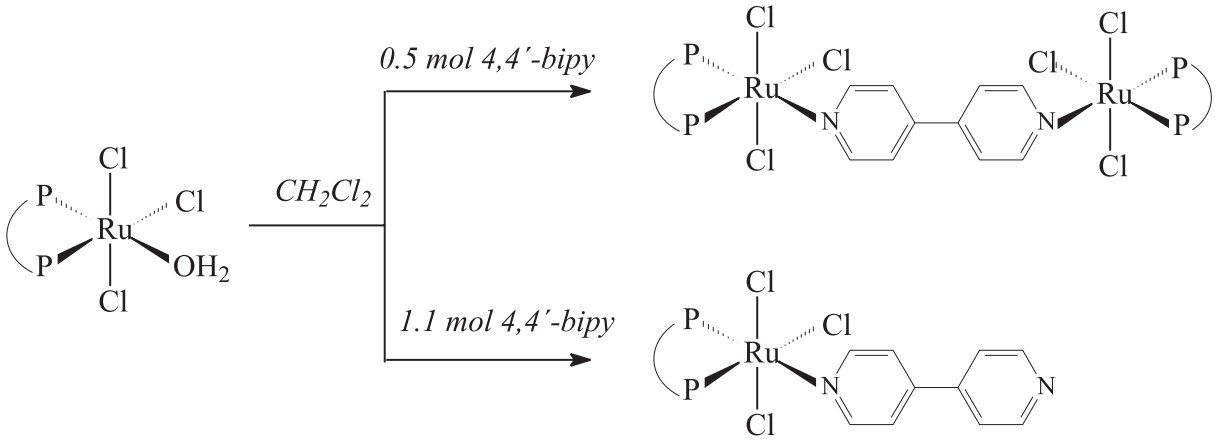

Scheme 1.

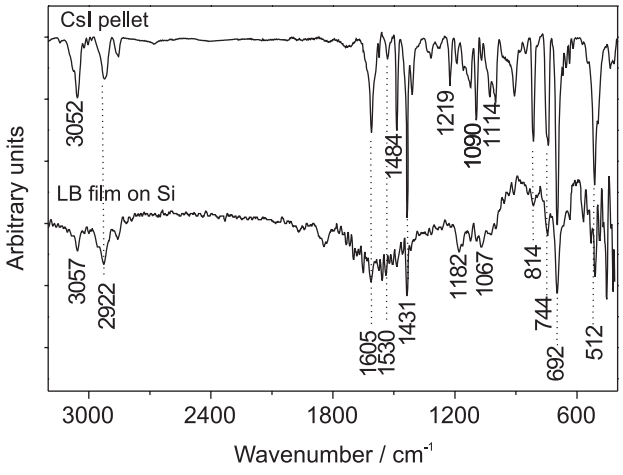

Figure 1. Transmission FTIR spectra for [{$RuCl_3$(dppb)}$_2$(μ-4,4'-bipy)] in a CsI pellet and 61-layer LB film transferred from pure water onto a Si wafer.

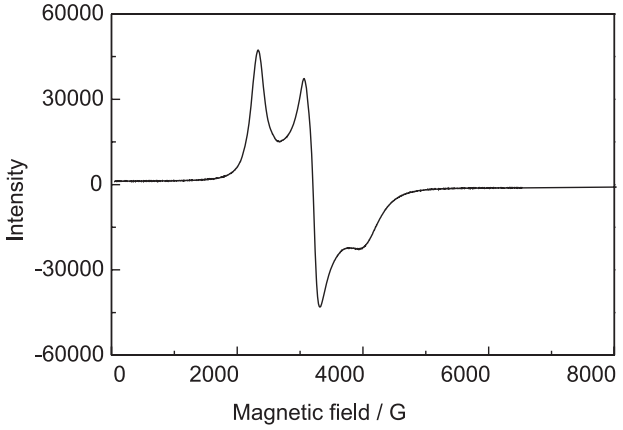

Figure 2. EPR spectrum of the [{$RuCl_3$(dppb)}$_2$(μ-4,4'-bipy)] (X band frequency) at -160 °C in the solid state.

The electronic spectrum of the [{$RuCl_3$(dppb)}$_2$(μ-4,4'-bipy)] in CH_2Cl_2 solution exhibits 3 bands in the visible region, as shown in Figure 3. The band at 328 nm may be assigned to allowed metal-to-ligand charge-transfer transition (MLCT), which corresponds to the electron transfer from the metal dπ orbital to the phosphorus (3πσ*dπ) orbitals of the dppb ligand. A low-intensity absorption band in similar position is also observed in the spectrum of [$Ru^{III}(PPh_3)_2(L)Cl_2$] (where L = 8-quinolinolate, 4-methyl-2-(phenylazo)phenolate or salicylal-diminate anion).[41] Based on systematic analyses of charge-transfer energies: (E_{MLCT} >> /E_{LMCT})[32], the band at 444 nm can be associated with electron transfer from the nitrogen atom (bipy) to the metal. The main band at 532 nm can be related to the transition from the chlorine orbitals to the metal [pπ (Cl^-)→ dπ (Ru^{III})].[42] The spectrum is similar to that observed for the d^5 ruthenium(III) compounds containing PPh_3, N-donors (pyridine, bipyridine, or phenanthroline), and Cl^- ligands,[43,44] and this spectrum corresponds closely to that of complex [$RuCl_3$(dppb)L] (L= pyridine) (see inset shown in Figure 3).[34]

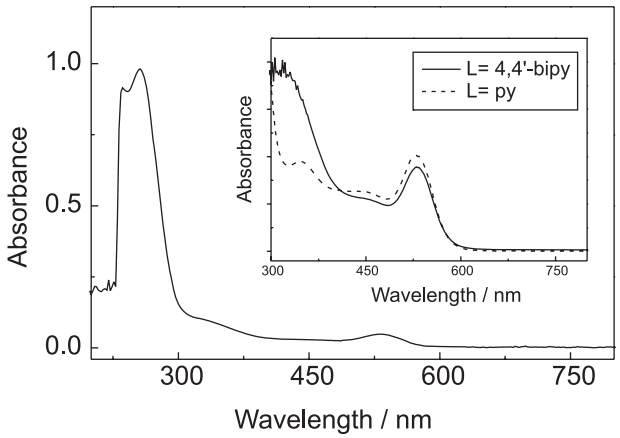

Figure 3. Electronic absorption spectra of [{$RuCl_3$(dppb)}$_2$(μ-4,4'-bipy)] in CH_2Cl_2 1×10^{-3} mol L^{-1} solution (solid line) and [$RuCl_3$(dppb)L] (L= pyridine) (dashed line), in CH_2Cl_2 1×10^{-4} mol L^{-1} solution.

Electrochemical characterization

Cyclic voltammograms of the [{$RuCl_3$(dppb)}$_2$(μ-4,4'-bipy)] complex in solution, at room temperature in CH_2Cl_2 with 0.1 mol L^{-1} of TBAP as supporting electrolyte, reveal an irreversible $Ru^{III/III}$ /$Ru^{III/II}$ process (only one electron involved), which is similar to that observed for [$RuCl_3$(dppb)L] (L= H_2O, dmso, pyridine and 4-methylpyridine) complexes.[33,34] In the first cycle starting at 0.30V, after inversion of the scan rate (at 1.0 V) a reduction process is observed at –0.23 V (peak 1 inside Figure 4). In the second cycle, two poorly defined oxidation processes appear, with Epa at 0.30 V and 0.41 V (peaks 2 and 3, respectively). This electrochemical behavior could be tentatively explained considering that with the reduction of $Ru^{III/III}$/$Ru^{III/II}$, at –0.23 V (in the first cycle), the species [(dppb)RuCl(μ-Cl)$_3$ClRu(dppb)] (equation 2), [$RuCl_2$(dppb)(4,4'-bipy)$_2$] (equation 3) and [$RuCl_2$(dppb)(μ-4,4'-bipy)]$_4$ (equation 4) could be generated at the electrode surface, according to Scheme 2. Then, the 1-1', 2-2' peaks could be assigned to the reduction of the Ru(III) center of mixed valence complex [(dppb)RuCl(μ-Cl)$_3$ClRu(dppb)], as confirmed by cyclic voltammetry on a chemically synthesized sample.[33,34] The 3-3´ peaks could be attributed to the [$RuCl_2$(dppb)(4,4'-bipy)$_2$] mononuclear complex and to the tetramer complex [$RuCl_2$(dppb)(μ-4,4'-bipy)]$_4$. The tetramer complex was isolated chemically by Queiroz *et al.*[38]

Monolayers at liquid-air interface

The surface pressure-area (π-A) isotherms of [{$RuCl_3$(dppb)}$_2$(μ-4,4'-bipy)] complex spread from $CHCl_3$

$$[Ru_2^{III/III}Cl_6(dppb)_2(\mu\text{-}4,4'\text{-bipy}) + e^- \rightarrow \text{“}[RuCl_3(dppb)]\text{”} + \text{“}[RuCl_2(dppb)(4,4'\text{-bipy})]\text{”} + Cl \quad (1)$$

$$\text{“}[RuCl_3(dppb)]\text{”} + \text{“}[RuCl_2(dppb)(4,4'\text{-bipy})]\text{”} \rightarrow [(dppb)RuCl(\mu\text{-}Cl)_3ClRu(dppb)] + 4,4'\text{-bipy} \quad (2)$$

$$\text{“}[RuCl_2(dppb)(4,4'\text{-bipy})]\text{”} + 4,4'\text{-bipy} \rightarrow [RuCl_2(dppb)(4,4'\text{-bipy})_2] \quad (3)$$

$$4\ \text{“}[RuCl_2(dppb)(4,4'\text{-bipy})]\text{”} \rightarrow [RuCl_2(dppb)(\mu\text{-}4,4'\text{-bipy})]_4 \quad (4)$$

Scheme 2.

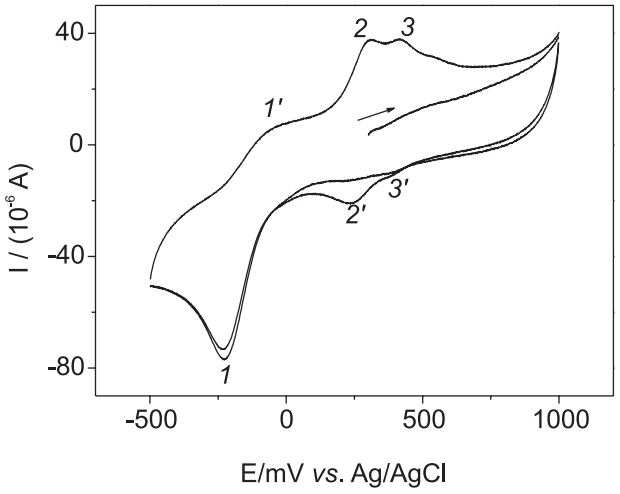

Figure 4. Cyclic voltammograms of $[\{RuCl_3(dppb)\}_2(\mu\text{-}4,4'\text{-bipy})]$, for potentials between -0.8 and 1.0 V, *vs*. Ag/AgCl, recorded in 1×10^{-3} mol L^{-1} in 0.1 mol L^{-1} TBAP in CH_2Cl_2; sweep rate 100 mV s^{-1}.

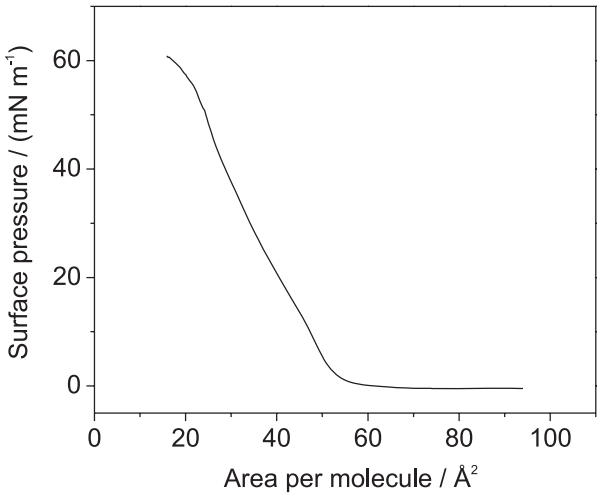

Figure 5. Surface pressure-area isotherm for $[\{RuCl_3(dppb)\}_2(\mu\text{-}4,4'\text{-bipy})]$ monolayer on ultra pure water subphase recorded at a compression speed of 10 mm min^{-1}, at 22 °C.

solutions onto pure water at 22 °C were recorded at several barrier compression rates. The mean area occupied by a molecule at monomolecular coverage at high pressures was determined by extrapolation at the condensed state to zero surface pressure. The value obtained was ~60 Å^2 and does not vary with compression speed. The isotherm in Figure 5 indicates that the complex begins to pack at an area per molecule of ~55 Å^2 and collapses at ~58 mN m^{-1}. From molecular modeling, two cross section areas were estimated for $[\{RuCl_3(dppb)\}_2(\mu\text{-}4,4'\text{-bipy})]$, viz. 272 Å^2 for the molecule lying on the plane (flat-on conformation) and 82 Å^2 for the molecule perpendicular to the plane (edge-on conformation). Therefore, the area per molecule obtained (60 Å^2) means that the molecules probably adopt an edge-on conformation, though formation of non-monomolecular structures is also possible, as observed for related complexes.[1,24,26,45,46] With the data presented herein, we cannot distinguish unequivocally between these 2 possibilities. Interestingly, the area accupied by the binuclear complex is twice the value for the related mononuclear complex, $[RuCl_3(dppb)L]$ (L= pyridine) (31 Å^2).[26]

Spectroscopic characterization of the LB films

The LB films were transferred at a surface pressure of 25 mN m^{-1} onto different substrates. For FTIR measurements, 61-layer LB films were transferred onto Si substrates that had been dried under vacuum. The spectrum shown in Figure 1 is similar to that of the powdered complex, with a slight difference at *ca*. 1100 cm^{-1}. This difference could be attributed to oxidation of the phosphorus ligand, which can occur due to interaction with water and/or air during fabrication of the Langmuir and LB films.[24]

The electronic absorption for a 31-layer LB film on a quartz substrate is shown in Figure 6, together with the spectra for $[\{RuCl_3(dppb)\}_2(\mu\text{-}4,4'\text{-bipy})]$ complex in solution and in a cast film. The latter was produced by dropping a saturated chloroform solution of the complex onto a quartz substrate, which was then dried under vacuum before use. The spectra of the solution and cast films are very similar, but differed considerably from that of the LB film. While the main absorption band of $[\{RuCl_3(dppb)\}_2(\mu\text{-}4,4'\text{-bipy})]$ in solution has a maximum at 532 nm, for the LB film a maximum in absorption occurs at 637 nm. This shift is indeed consistent with the

different colors exhibited by the samples, which is bluish-green for the organized LB film and red for the cast film and solution. Similar result was observed for [$RuCl_3$(dppb)L] (L= 4-methylpyridine),[24] from which we can infer that this colour change is caused by oxidation of the bisphosphine group, thus corroborating the FTIR characterization described above.

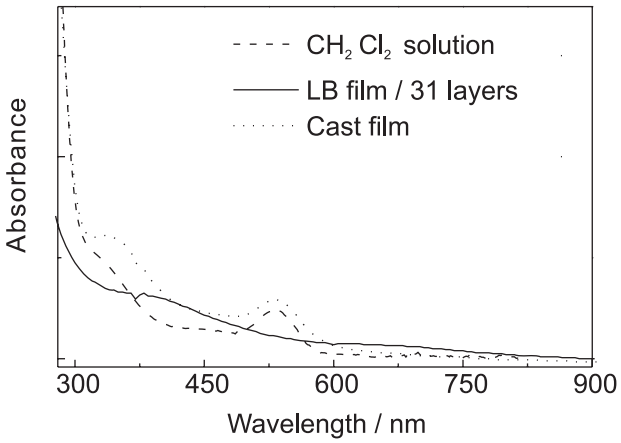

Figure 6. Electronic absorption spectra for [{$RuCl_3$(dppb)}$_2$(μ-4,4'-bipy)] in CH_2Cl_2 1×10^{-3} mol L^{-1} solution (dashed line), for a 31-layer LB film transferred from pure water subphase onto quartz (solid line), and for a cast film (dotted line).

Electrochemical characterization of the LB films

Understanding the electrochemical properties of LB films is essential for applications in sensors. The cyclic voltammograms of a 31-layer LB film from [{$RuCl_3$(dppb)}$_2$(μ-4,4'-bipy)] deposited onto ITO are shown in Figure 7. For a sweeping rate of 30 mV s^{-1} an anodic peak appears at Epa = 0.41 V, with a cathodic peak at Epc of 0.27 V (less defined) *vs*. Ag/AgCl 0.5 mol L^{-1} KCl (pH 1.0), which are attributed to the $Ru^{III}Ru^{III}$ / $Ru^{II}Ru^{II}$ redox process. The peak current (i_{pa} and i_{pc}) increased linearly with the square root of the scan rate ($v^{1/2}$) (R= 0.99927), as illustrated in the inset of Figure 7. Additionally, the oxidation (reduction) peak potential shifted to more positive (negative) values with the increase in scan rate. These two observations indicate a quasi-reversible redox process.[47] The increase in peak to peak separation for higher scan rates may be associated to redox processes occuring, not only on superficial species, but also with molecules inside the film. Therefore, ions from the solution must migrate to the film to compensate for charge created. However, the ion diffusion inside the film is slower than in solution. Thus, at higher scan rates an extra over-potential is necessary to reach the diffusional limit for the peak current. The supporting electrolyte at pH 1.0 was used because a previous study with electrolyte solutions at

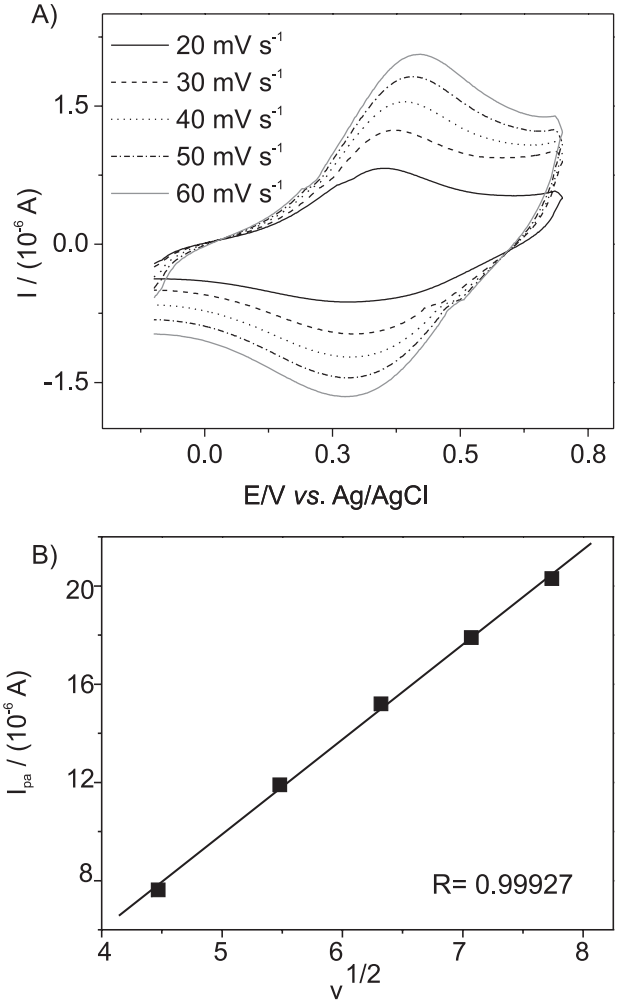

Figure 7. (a) Cyclic voltammograms of [{$RuCl_3$(dppb)}$_2$(μ-4,4'-bipy)], for potentials between -0.1 and 0.7 V, *vs*. Ag/AgCl, for a 31-layer LB film transferred from pure water onto ITO; sweep rate 30 mV s^{-1}; (b) Peak current (Ipa) *vs*. $v^{1/2}$ for the 31-layer LB film.

different pHs best responses (with higher peak current values) were obtained below pH 3 (results not shown).

In addition to investigating LB films, we also studied the electrochemical properties of cast and dip coated films. The electrochemical behavior of the films from [{$RuCl_3$(dppb)}$_2$(μ-4,4'-bipy)] is considerably different from that of the complex in solution, as indicated in Figures 5, 7 and 8. This occurs since with the reduction of Ru^{III} of the [{$RuCl_3$(dppb)}$_2$(μ-4,4'-bipy)] in solution at -0.23 V, in the first cycle, new species are generated at the electrode surface, according to Scheme 2 proposed in this work. The differences in the voltammetric profiles of the LB films and the complex solution may be attributed to the immobilization of ruthenium on the solid surface, which impairs the formation of mono- and binuclear metallic species that occur in solution. Therefore, only the redox process associated with the metallic center can

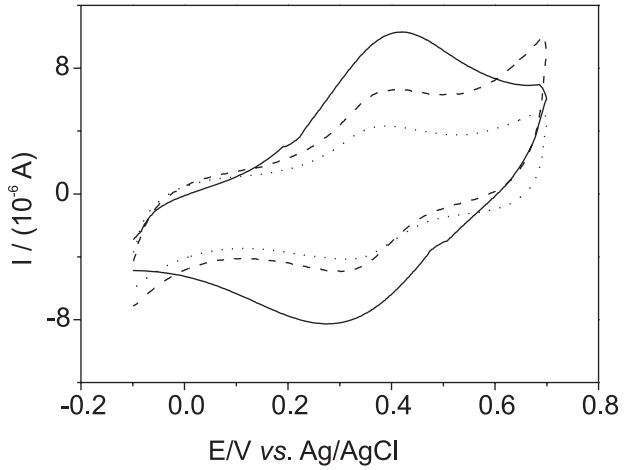

Figure 8. Cyclic voltammograms of [{$RuCl_3$(dppb)}$_2$(μ-4,4'-bipy)], for potentials between -∂0.1 and 0.7 V, *vs*. Ag/AgCl, recorded for a 31-layer LB film (solid line), cast film (dashed line), dip coated film (dotted line); sweep rate 30 mV s^{-1}.

occur. Same results were observed for [$RuCl_3$(dppb)L] (L= 4-methylpyridine).[48]

The effects of the organized structure of LB films are manifested in the electrochemical properties. The cast and dip coated films exhibited closer values of anodic and cathodic potentials (cast film: at Epa = 0.38 V and Epc= 0.32 V; dip coated film: Epa = 0.39 V and Epc= 0.31 V), in comparison to the LB film (Epa = 0.41 V and Epc= 0.27 V). The difference in redox processes should be attributed to the phase separation and formation of aggregates onto ITO, in contrast to the LB film.[4] Peak currents for the LB films were higher (Ipa = 10 μA and Ipc= -8 μA) than for the cast (Ipa = 4 μA and Ipc= -4 μA) and dip coated films (Ipa = 6 μA and Ipc= -5 μA). This increase is probably due to the layer-by-layer, ordered structure of the LB film. Moreover, the electroactivity of the LB films also points to the possibility of employing [{$RuCl_3$(dppb)}$_2$(μ-4,4'-bipy)] films in electrochemical devices.

Conclusions

The binuclear complex [{$RuCl_3$(dppb)}$_2$(μ-4,4'-bipy)] was successfully prepared as demonstrated with elemental analysis. The complex *mer*-[$RuCl_3$(dppb)].H_2O used as starting material in this synthesis is a versatile precursor for coordination compounds containing the Ru^{III}P-P core. The complex is soluble in weakly polar organic solvents, thus facilitating studies using the Langmuir-Blodgett method. The binuclear complex formed stable monolayers, with molecular area (*ca*. 60 $Å^2$) smaller than expected. In solution the binuclear complex displayed considerably different behavior of the LB film, in terms of spectroscopic and electrochemical properties. The LB films exhibited a green-bluish color, instead of the red color observed in solution, which is attributed to oxidation of the phosphine ligands. In spite of the similarity of the absorption spectra of the solution and the cast film, the redox properties of the latter resembled more those of the LB film. This was ascribed to the immobilization of ruthenium on the solid surface, which impairs the formation of binuclear and polinuclear species occurring in solution. Nevertheless, the LB films presented larger peak currents, probably due to the organized nature provided by the Langmuir-Blodgett technique.

Acknowledgments

The financial support from CNPq, FAPESP, IMMP-CNPq and Fundação Araucária (Brazil) is gratefully acknowledged.

References

1. Ryan, M.F.; Metcalfe, R.A.; Lever, A.B.P.; Haga, M-a.; *J. Chem. Soc., Dalton Trans.* **2000**, 2357.
2. DeArmoond, M.K.; Fried, G.; *Prog. Inorg. Chem*. **1997**, *44*, 97.
3. Ferreira, M.; Dinelli, L.R.; Wohnrath, K.; Batista, A.A.; Oliveira Jr., O.N.; *Thin Sol. Films* **2004**, *446*, 301.
4. Wohnrath, K.; Pessoa, C.A.; dos Santos, P.M.; Garcia, J.R.; Batista, A.A.; Oliveira Jr., O.N.; *Prog. Sol. State Chem.* **2005**, *33*, 243.
5. Santos, J.P.; Zaniquelli, M.E.; Batalani, C.; De Giovani, W.F.; *Thin Sol. Films* **2001**, *105,* 1780.
6. Wang, K.; Haga, M.; Hossain, M.D.; Shindo, H.; Hasebe, K.; Monjushiro, H.; *Langmuir* **2002**, *18* , 3528.
7. Ferreira, M.; Constantino, C.J.L.; Riul Jr., A.; Wohnrath, K.; Aroca, R.F.; Giacometti, J.A.; Oliveira Jr., O.N.; Mattoso, L.H.C.; *Polymer* **2003**, *44*, 4205.
8. Ferreira, M.; Riul Jr., A.; Wohnrath, K.; Fonseca, F.J.; Oliveira Jr., O.N.; Mattoso, L.H.C.; *Anal. Chem.* **2003**, *75,* 953.
9. Riul Jr., A.; dos Santos, D.S.; Wohnrath, K.; Di Tommazo, R.; Carvalho, A.C.P.L.F.; Fonseca, F.J.; Oliveira Jr., O.N.; Taylor, D.M.; Mattoso, L.H.C.; *Langmuir* **2002**, *18,* 239.
10. Lu, W.X.; Zhou, H.L.; He, P.S.; Guo, W.H.; *Thin. Sol. Films* **2000**, *365*, 67.
11. Fujihira, M. Yanagisawa, M.; Kondo, T.; Suga, K. *Thin. Sol. Films* **1992**, *210/211*, 265.
12. Taniguchi, T.; Fukasawa, Y.; Miyashita, T.; *J. Phys. Chem. B* **1999**, *103*, 1920.
13. Miller, C.J.; Bard, A.J.; *Anal. Chem*. *1991*, **63**, 1707.
14. Kalyanasundaram, K.; *Coor. Chem Rev.* **1982**, *46*, 159.
15. Marmion, M.E.; Takeuchi, K.J.; *J. Am. Chem. Soc.* **1988**, *110*, 1472.

16. Parshall, G.W.; Ittel, S.D.; *Homogeneous Catalysis*, John Wiley & Sons: New York, 1992.
17. Naota, T.; Takaya, H.; Murahashi, S.-I.; *Chem. Rev.* **1998**, *98*, 2599.
18. Queiroz, S.L.; Batista, A.A.; *Quim. Nova* **1994**, *94*, 1239.
19. De Armond, M.K.; Fried,G.A.; *Prog. Inorg. Chem.* **1997**, *44*, 97.
20. Kakkar, A.K.; *Chem. Rev.* **2002**, *102*, 3579.
21. Roberts, G. G.; *Langmuir-Bldgett Films*; Plenum Press: New York, 1990.
22. Ulman, A.; *An Introduction to Ultrathin Organic Films*: *From Langmuir-Blodgett to Self-Assembly*; Harcourt Brace Jovanivich: Boston, 1991.
23 Ghadiri, M. R.; Granja, J. R.; Milligan, R. A.; McRee, D. E.; Khazanovich, N.; *Nature* **1993**, *366*, 324.
24. Wohnrath, K.; Constantino, C.J.L.; Antunes, P.A.; Santos, P.M.; Batista, A.A.; Aroca, R.F.; Oliveira Jr., O.N.; *J. Phys. Chem. B* **2005**, *109,* 4959.
25. Ferreira, M.; Zucolotto, V.; Ferreira, M.; Oliveira Jr., O.N.; Wohnrath, K. In *Encyclopedia of Nanoscience and Nanotechnology*; Nalwa H.S. ed.; American Scientific Publishers: Valencia, CA, 2004, vol.4.
26. Ferreira, M.; Wohnrath, K.; Riul Jr., A.; Giacometti, J.A.; Oliveira Jr., O.N.; *J. Phys. Chem. B* **2002**, *106,* 7272.
27. Ferreira, M.; Wohnrath, K.; Torresi, R.M.; Constantino, C.J.L.; Aroca, R.F.; Oliveira Jr., O.N.; Giacometti, J.A.; *Langmuir* **2002**, *18,* 540.
28. Wohnrath, K.; Mello, S.V.; Pereira-da-Silva, M.A.; Oliveira Jr., O.N.; *Synt. Metals* **2001**, *121,* 1426.
29. De Araujo, M.P.; Porcu, O.M.; Batista, A.A.; Oliva, G.; Souza, D.H.F.; Bonfadini, M.; Nascimento, O.R.; *J. Coord. Chem*. **2001**, *54*, 81.
30. Rocha, R.C.; Toma, H.E.; *Quim. Nova* **2002**, *25*, 624.
31. Rocha, R.C.; Toma, H.E.; *Polyhedron* **2002**, *21*, 2089.
32. Rocha, R.C.; Toma, H.E.; *Polyhedron* **2003**, *22*, 1303.
33. Dinelli, L.R.; Batista, A.A.; Wohnrath, K.; Araujo, M.P.; Queiroz, S.L.; Bonfadini, M.R.; Oliva, G.; Nascimento, O.R.; Cyr, P.; MacFarlane, K.; James, B.R.; *Inorg. Chem*. **1999**, *38*, 5341.
34. Wohnrath, K.; Araujo M.P.; Dinelli, L.R.; Batista, A.A.; Moreira, I.S.; Castellano, E.E.; Ellena, J.; *J. Chem. Soc., Dalton Trans*. **2000**, 3383.
35. Araujo, M. P.; Valle, E. M.A.; Ellena, J.; Castellano, E.E.; dos Santos, E.N.; Batista, A. A.; *Polyhedron* **2004**, *23*, 3163.
36 Santiago, M.O.; Sousa, J.R.; Diógenes, I.C.N.; Lopes, L.G.F.; Meyer, E.; Castellano, E.E.; Ellena, J.; Batista, A.A.; Moreira, I.S.; *Polyhedron* **2006**, *25*, 1543.
37. Silva a, A.L.R.; Santiago, M.O.; Diógenes, I.C.N.; Pinheiro, S.O.; Castellano, E.E.; Ellena, J. Batista, A.A.; do Nascimento, F.B.; Moreira, I.S.; *Inorg. Chem. Comm.* **2005**, *8*, 1154.
38. Queiroz, S.L.; Kikuti, E.; Ferreira, A.G.; Santiago, M.O.; Batista, A.A.; Castellano, E.E.; Ellena, J.; *Supramolecular Chem*. **2004**, *16*, 255.
39. Batista, A. A.; Polato, E. A.; Queiroz, S. L.; Nascimento, O. R.; James, B. R.; Rettig, S. J.; *Inorg. Chim. Acta* **1995**, *230,* 111.
40. Bag, N.; Lahiri, G.K.; Chakravorty, A.J.; *J. Chem. Soc., Dalton Trans.* **1990**, 1557.
41. Sinha, P.K.; Chakravarty, J.; Bhattacharya, S.; *Polyhedron* **1997**, *16*, 81.
42. Duff, C. M.; Heath, G. A.; *J. Chem. Soc., Dalton Trans.* **1991**, 2041.
43. Wajda-Hermanowicz, K.; Ciunik, Z.; Kochel, A.; *Inorg. Chem.* **2006**, 45, 3369.
44. Ruiz-Ramirez, L.; Stephenson, T.A.; Switkes, E.S.; *J Chem. Soc., Dalton Trans.* **1973**, 1770.
45. Richardson, T.; Roberts, G.G.; Barghout, R.; Compton, R.G.; Riley, D.J.; *Electroanalysis* **1985**, *89*, 5698.
46. Fu, Y.; Forman, M.; Leznoff, C.C.; Lever, A.B.P.; *J. Phys. Chem.***1994**, *98,* 8985.
47. Bard, A.J.; Faulkner,L.R.; *Electrochemical Methods Fundamentals and Applications*, John Wiley & Sons: New York, 1980.
48. Wohnrath, K.; Garcia, J.R.; Nart, F.C.; Batista, A.A.; Oliveira Jr., O.N.; *Thin Sol. Films* **2002**, *402,* 272.

Received: June 16, 2006
Published on the web: December 4, 2006

FAPESP helped in meeting the publication costs of this article.